Theoretical Models and Experimental Data for Reactions between Water and Protonated Alcohols: Substitution and Elimination Mechanisms

Einar Uggerud* and Lihn Bache-Andreassen[a]

Abstract: The substitution reactions: $H_2{}^*O + R{-}OH_2^+ \rightarrow R{-}{}^*OH_2^+ + H_2O$ and elimination reactions: $H_2{}^*O + R{-}OH_2^+ \rightarrow (R{-}H) + (H_2O \cdot H_2{}^*O)H^+$ [$R = CH_3$, CH_3CH_2, $(CH_3)_2CH$, and $(CH_3)_3C$; $(R{-}H) =$ alkene] have been studied at low pressure in a Fourier transform ion cyclotron resonance mass spectrometer, and modelled with quantum-chemical methods and microcanonical variational transition state theory. The relative rates of the substitution reactions are $(CH_3)_3C > (CH_3)_2CH > CH_3 > CH_3CH_2$; this is in good agreement with the theoretical calculations. This is different from the situation in solution in which the trend $CH_3 > CH_3CH_2 > (CH_3)_2CH > (CH_3)_3C$ traditionally is explained by the notion that increased methyl substitution at the α-carbon reduces the rate constant for S_N2 reactions owing to increased steric hindrance. For $R = (CH_3)_2CH$ and $(CH_3)_3C$ front-side nucleophilic substitution and elimination are competing with back-side S_N2. Both these barriers decrease upon increased methyl substitution at the α carbon. The carbocationic character of all key transition structures and intermediates becomes more prevalent upon increased methyl substitution. Ab initio calculations with additional water molecules (to mimic water solvation) illustrate the origin of the differences in reactivity in the gas phase and solution.

Keywords: ab initio calculations · cluster compounds · eliminations · mass spectrometry · nucleophilic substitutions

Introduction

Alcohols hydrolyze in aqueous acidic media to give re-formed alcohols by water exchange and alkenes by water elimination.[1] The product distributions depend on the structural features of the alcohol and the nature of the medium (in particular the acid concentration). The mechanisms of these and related ionic nucleophilic-substitution and elimination reactions have been studied extensively and systematically for more than a hundred years.[2–4] Sixty years ago, Ingold and coworkers made their important and fruitful contribution to our understanding of these classes of reactions by introducing the mechanistic concepts S_N1, S_N2, E1 and E2.[5] These concepts are familiar to most chemists, but it is useful for the rest of the discussion to have them clearly defined within the framework used here. The basic difference between S_N1 and S_N2 is exemplified by consideration of the following reaction schemes for reactions between a nucleophile ($H_2{}^*O$, labelled for convenience) and a protonated alcohol molecule ($R{-}OH_2^+$), Equations (1) and (2).

[a] Prof. Dr. E. Uggerud, L. Bache-Andreassen
Department of Chemistry, University of Oslo
PO Box 1033, Blindern, N-0315 Oslo (Norway)
Fax: (+47) 22-85-54-41
E-mail: einar.uggerud@kjemi.uio.no

$$R{-}OH_2^+ \longrightarrow R^+ + H_2O \quad (1a)$$

$$R^+ + H_2{}^*O \longrightarrow R{-}{}^*OH_2^+ \quad (1b)$$

$$H_2{}^*O + R{-}OH_2^+ \longrightarrow R{-}{}^*OH_2^+ + H_2O \quad (2)$$

Reaction 1 is an S_N1 reaction. The bond between the leaving group (OH_2) and the rest of the substrate molecule (R^+) is completely broken before the bond between R^+ and the nucleophile ($H_2{}^*O$) starts to form. The intermediate existence of a carbocation, R^+, is a key issue, and the rate-determining step is unimolecular. Reaction 2 is an S_N2 reaction. In this mechanism the nucleophile attacks from the end opposite to that of the leaving group and the new bond is formed gradually as the old bond is broken (Scheme 1). The rate determining step is bimolecular, there is no intermediate carbocation, a single transition state is passed, and the mechanism explains why inversion of configuration around the central carbon atom (Walden inversion) is usually observed when the reaction follows this mechanism.

Although this picture still is generally accepted, it has been modified and refined over the years. One difficulty with the original Ingold scheme is that many solvolysis reactions that apparently are S_N1 do not give completely racemic product mixtures as expected.[6] The existence of a free long-lived intermediate carbocation would permit nucleophilic attack

  0947-6539/99/0506-1917 $ 17.50+.50/0

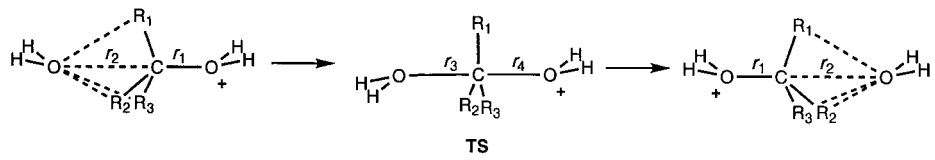

Scheme 1. Schematic representation of the S_N2 mechanism for the reaction between water and protonated alcohols.

from either face of the planar carbocation with equal probability. In order to take the role of the reaction medium more explicitly into account, Winstein and co-workers introduced the idea of stepwise dissociation of the reactant molecule (R^+, OH_2) of decreasing tightness during the S_N1 series of events.[7]

Another problem is that a given set of reactants may give rise to different reaction characteristics (S_N1 or S_N2) depending on the conditions.[4, 8] One way to explain this situation is to operate on a mechanistic sliding scale; no reaction is purely S_N1 or S_N2, but somewhere in-between.[9–11] The exact position on the sliding scale is determined by the reaction conditions. A completely different explanation is that the distinct S_N1 and S_N2 mechanisms always operate in parallel.[11–13] The reaction conditions determine to what extent which one predominates.

The postulated existence of short-lived carbocations in the S_N1 and in the analogous E1 mechanisms is an essential point which deserves a comment at this stage of the discussion. The existence of alkyl carbocations with the general formula $C_nH_{2n+1}^+$ ($n = 1, 2, 3,\ldots$) in the gas phase has been verified repeatedly, both experimentally[14] and by precise quantum-chemical calculations.[15, 16] The existence of practically free carbocations has also been demonstrated in solution under given conditions.[17] In strongly acidic (super-acid) solutions and in the absence of nucleophiles, propyl and butyl carbocationic species have been observed by NMR, IR and ESCA (electron spectroscopy for chemical analysis). The smaller methyl and ethyl cations remain unobserved in super-acid. The question whether free carbocations really exist under the conditions in which S_N1 is the claimed mechanism is perhaps more a problem of semantics than a chemical one. As we shall point out in this paper, the key points are the lifetime of the intermediate carbocation,[11] the dynamics of formation of the carbocationic species, and the nature of the interaction between the carbocation and the surrounding molecules.

The purpose of this work is to uncover the intrinsic properties of the reactants, intermediates, transition structures, and products during solvolysis of simple aliphatic alcohols in acidic water. We have chosen to pursue this by isolating the reactants in the gas phase at very low pressures. Under such conditions solvent effects are inoperative. In addition we wanted to study the effects of successive addition of water molecules to the reaction system to bridge the reactivity in the gas phase with that in solution. We present the results from experiment and extensive calculations of the reactions of protonated methanol, ethanol, *iso*-propanol and *tert*-butanol with water, and with water embedded in clusters of two or four extra water molecules. The alcohols were chosen in order to systematically uncover the effect of substituting hydrogens with methyl groups, and because the corresponding alkyl groups are stable with respect to isomerization. A key point of this study is that the reactants and products are identical. This means that the reaction exothermicity is zero, and that the intrinsic properties of the nucleophile/nucleofuge and the substrate are directly probed.[18] The great advantage of the small scale models examined is that the mechanistic concepts of a transition state and an intermediate have precise mathematical definitions within the framework of the potential energy function of the molecular super system.[19] Among the many questions we try to answer are the following:

1) What role do free carbocations play in the reactions?
2) How do the barrier heights depend on the structure of the alkyl group?
3) How applicable are cluster models to the solution-phase chemistry of the systems examined?

Abstract in Norwegian: *De bimolekylære substitusjonsreaksjonene: $H_2{*}O + R{-}OH_2^+ \rightarrow R{-}{*}OH_2^+ + H_2O$ og eliminasjonsreaksjonene: $H_2{*}O + R{-}OH_2^+ \rightarrow (R{-}H) + (H_2O \cdot H_2{*}O)H^+$ [$R = CH_3$, CH_3CH_2, $(CH_3)_2CH$, og $(CH_3)_3C$; $(R{-}H)$ = alken] har blitt studert ved hjelp av et fouriertransformasjon-ionesyklotronresonans massespektrometer, og modellert ved bruk av kvantekjemiske metoder og mikrokanonisk variasjonell overgangstilstandsteori. De relative reaksjonshastighetene til substitusjonsreaksjonene er $(CH_3)_3C > (CH_3)_2CH > CH_3 > CH_3CH_2$, noe som er i god overensstemmelse med de teoretiske beregningene. Dette er annerledes enn situasjonen i løsning hvor rekkefølgen $CH_3 > CH_3CH_2 > (CH_3)_2CH > (CH_3)_3C$ tradisjonelt forklares med at økt metylsubstitusjon på α-karbonet reduserer reaksjonshastigheten for S_N2-reaksjoner grunnet økt sterisk hindring. For $R = (CH_3)_2CH$ og $(CH_3)_3C$ finner også eliminasjon sted, og de teoretiske beregningene viser at en forside-angrep nukleofil substitusjonsmekanisme også konkurrerer med bakside-angrep S_N2. Barrierene for eliminasjon og forside-angrep substitusjon synker med økt metylsubstitusjon på α-karbonet, mens barrierene for bakside-angrep substitusjon synker i motsatt rekkefølge av reaksjonshastighetene. Den karbokationiske karakteren til alle viktige overgangstilstander og intermediater blir mer fremtredene med økt metylsubstitusjon. Ab initio beregninger med flere vannmolekyler (for å etterlikne situasjonen i løsning) illustrerer opphavet til reaktivitetsforskjellene i gassfase og i løsning.*

Methods

Mass spectrometric experiments: The reactions were studied with a Fourier transform ion cyclotron resonance (FT-ICR) mass spectrometer equipped with an external ion source (Apex 47e, Bruker Daltonics, Billerica, Massachusetts, USA). The protonated alcohols, ROH_2^+, were generated by proton transfer to the corresponding alcohols under chemical ionization

0947-6539/99/0506-1918 $ 17.50+.50/0 *Chem. Eur. J.* **1999**, *5*, No. 6

(CI) conditions in the external ion source. For protonated methanol, ethanol, and *iso*-propanol, methane was used as the CI gas, while for protonated *tert*-butanol the CI gas was *iso*-butane. The mixture of ions produced in the external source was transferred to the ICR cell. The cell contained labelled water ($H_2{}^{18}O$) at a stationary partial pressure in the range $1.4\times10^{-8}-4.0\times10^{-7}$ mbar. The temperature of the cell wall was estimated to be approximately 300 K. All ions with m/z values different from that of the ion of interest (ROH_2^+) were then ejected from the cell by correlated frequency sweep.[20] Subsequently argon was introduced into the cell by means of a pulsed valve (peak pressure 10^{-5} mbar) and then allowed to pump away for 3–4 seconds. During this period the multiple collisions between the trapped ions and argon ensured that the ions were thermally and translationally cooled to ambient conditions before they were used. After this event, isolation of the ROH_2^+ ions was accomplished either by single-frequency shots or correlated frequency sweep to remove unwanted ions. This was necessary because small amounts of ionic reaction products and ionic fragments, formed by collisionally induced decomposition, are produced during the cooling period. The reactions were observed by recording mass spectra after a variable reaction time, t_r. In this way the product ion distribution could be obtained as a function of time. Second-order rate constants for the total consumption of the reactant ions were determined from the slope of the straight line obtained by plotting the logarithm of the normalized reactant-ion intensities against t_r. The high degree of linearity of the plots demonstrated that the reactant ions were translationally and thermally equilibrated as a result of their careful preparation. All measurements were repeated on at least four separate occasions to ensure long-time reproducibility and to obtain reliable measurement statistics. The ion gauge was calibrated by measurement of the reaction rate for Equation (3) ($k_3=2.2\times10^{-9}$ cm^{3}molecule^{-1}s^{-1}).[21] The instrument was operated at sufficiently high resolution to identify all reactants and products by precise mass measurement. Chemicals were of research quality and were checked for purity by mass spectrometry before use.

$$NH_3{}^{+\cdot}+NH_3 \longrightarrow NH_4^+ + NH_2^{\cdot} \quad (3)$$

Quantum-chemical model calculations: Quantum-chemical calculations were carried out by means of the program systems GAUSSIAN 94.[22] The basis set 6-31G(d)[23, 24] was employed. The quantum-chemical methods used were Hartree–Fock (HF),[25] second-order Møller–Plesset perturbation theory (MP2)[26] and the hybrid-density functional theory as developed by Becke (B3LYP).[27] All relevant critical points (reactants, transition structures, intermediates and products) of the potential-energy surface were characterized by complete optimization of the molecular geometries for HF/6-31G(d) and the respective MP2/6-31G(d) single-point energies were computed for these geometries. In the following, these methods will be designated by the abbreviations HF and MP2//HF. Except for the clusters, MP2/6-31G(d) and B3LYP/6-31G(d) geometries were completely optimized. These methods are designated MP2 and B3LYP. Harmonic frequencies were obtained by diagonalizing the mass-weighted Cartesian force-constant matrix, calculated from the analytic second derivatives of the total energy (the Hessian). Harmonic frequencies obtained in this manner were used to calculate the zero-point vibrational energies (zpve) as described below. Relative energies were calculated by including the zero-point vibrational energies scaled by factors of 0.9135 (HF/6-31G(d)), 0.9670 (MP2/6-31G(d)) and 0.9806 (B3LYP/6-31G(d)).[28] Where nothing else is indicated, properties which are discussed in the text are from the MP2 calculations. To calculate rate constants for the ion-molecule reactions a microcanonical variational Rice–Ramsperger–Kassel–Marcus (RRKM) method[29, 30] as implemented by Brauman and co-workers[31] was employed. The computer program used (HYDRA) was obtained from these authors. Structural parameters and scaled harmonic vibration frequencies for reactants, intermediates, and transition states were taken from the MP2 calculations (vide infra). A complete list of energy data and cartesian coordinates of the structures may be obtained from the authors.

Results and Discussion

Reactions between water and protonated alcohols: The substitution reaction [Eq. (4)] was observed to occur very slowly, and the product and reactant ion mixture had to be monitored up to 240 s before the reactant was completely consumed. Trace amounts of methanol and ammonia were present in the background, each with a partial pressure of 5×10^{-9} mbar or less. This gave rise to the competing reactions, Equations (5) and (6).

$$H_2{}^{18}O + CH_3OH_2^+ \ (m/z=33) \longrightarrow CH_3{}^{18}OH_2^+ \ (m/z=35) + H_2O \quad (4)$$

$$CH_3OH + CH_3OH_2^+ \longrightarrow (CH_3)_2OH^+ \ (m/z=47) + H_2O \quad (5)$$

$$NH_3 + \{CH_3{}^{18}OH_2^+ \text{ or } CH_3OH_2^+ \text{ or } (CH_3)_2OH^+\} \longrightarrow NH_4^+ \ (m/z=18) + \{CH_3{}^{18}OH \text{ or } CH_3OH \text{ or } (CH_3)_2O\} \quad (6)$$

Ammonia acted as a proton sink in the total reaction system owing to its high proton affinity. In order to obtain the rate constants for reaction in Equation (4), the reactions in Equations (5) and (6) had to be taken explicitly into account during analysis of the kinetic data. By means of standard curve-fitting methods, we determined the second-order rate constant for the reaction in Equation (4) to be $k_4=2.2\times10^{-13}$ cm^{3}molecule^{-1}s^{-1}. The uncertainty in this figure is mainly due to the error in the pressure determination and was estimated to be $\pm20\,\%$. However, when compared with the other rate constants reported in this paper, the relative uncertainty is less than $\pm10\,\%$ (2 standard deviations).

The reaction between labelled water and protonated ethanol is even slower and gave only one major reaction product [Eq. (7)]. The elimination reaction was also observed [Eq. (8)], but was too slow for precise measurement. In this case ethanol was present in the cell at a partial pressure of approximately 5×10^{-9} mbar and the competing reaction was observed [Eq. (9)].

$$H_2{}^{18}O + CH_3CH_2OH_2^+ \ (m/z=47) \longrightarrow CH_3CH_2{}^{18}OH_2^+ \ (m/z=49) + H_2O \quad (7)$$

$$H_2{}^{18}O + CH_3CH_2OH_2^+ \ (m/z=47) \longrightarrow (H_2{}^{18}O)(H_2O)H^+ \ (m/z=39) + CH_2CH_2 \quad (8)$$

$$CH_3CH_2OH + CH_3CH_2OH_2^+ \longrightarrow (CH_3CH_2)_2OH^+ \ (m/z=75) + H_2O \quad (9)$$

This reaction and proton transfer to ammonia were incorporated into the kinetic scheme and the rate constant $k_7=6.7\times10^{-14}$ cm^{3}molecule^{-1}s^{-1} was obtained by curve fitting. We estimate the rate constant for the elimination reaction to be $k_8<1.0\times10^{-15}$ cm^{3}molecule^{-1}s^{-1}.

In the case of protonated *iso*-propanol the situation was slightly more complicated. In addition to the substitution product a substantial peak was observed for the proton-bonded water dimer showing the occurrence of elimination. A small peak due to the formation of $C_3H_7^+$ was also detected, Equations (10)–(12). The reactions given in Equations (13)–16) were also observed and taken into consideration.

$$H_2{}^{18}O + (CH_3)_2CHOH_2^+ \ (m/z=61) \longrightarrow (CH_3)_2CH^{18}OH_2^+ \ (m/z=63) + H_2O \quad (10)$$

$$H_2{}^{18}O + (CH_3)_2CHOH_2^+ \longrightarrow (H_2{}^{18}O)(H_2O)H^+ \ (m/z=39) + CH_3CHCH_2 \quad (11)$$

$$H_2{}^{18}O + (CH_3)_2CHOH_2^+ \longrightarrow (CH_3)_2CH^+ \ (m/z=43) + (H_2{}^{18}O)(H_2O) \quad (12)$$

$$(CH_3)_2CHOH + (CH_3)_2CHOH_2^+ \longrightarrow ((CH_3)_2CH)_2OH^+ \ (m/z = 103) + H_2O \quad (13)$$

$$H_2{}^{18}O + (H_2{}^{18}O)(H_2O)H^+ \longrightarrow (H_2{}^{18}O)_2H^+ \ (m/z = 41) + H_2O \quad (14)$$

$$(CH_3)_2CHOH + (H_2{}^{18}O)_2H^+ \longrightarrow ((CH_3)_2CHOH)(H_2{}^{18}O)H^+ \ (m/z = 81) + H_2{}^{18}O \quad (15)$$

$$(CH_3)_2CHOH + ((CH_3)_2CHOH)(H_2{}^{18}O)H^+ \longrightarrow ((CH_3)_2CHOH)_2H^+ \ (m/z = 121) + H_2{}^{18}O \quad (16)$$

In addition some proton transfer to ammonia was observed. With this model the rate constants for the substitution and elimination reactions were estimated by curve fitting to be $k_{10} = 4.6 \times 10^{-11}\ cm^3\,molecule^{-1}\,s^{-1}$, $k_{11} = 1.4 \times 10^{-11}\ cm^3\,molecule^{-1}\,s^{-1}$ and $k_{12} = 1.1 \times 10^{-12}\ cm^3\,molecule^{-1}\,s^{-1}$ for reactions (10–(12), respectively.

In the reaction between labelled water and protonated *tert*-butanol both substitution and elimination were observed, Equations (17)–(19). Protonated water-dimer formation

$$H_2{}^{18}O + (CH_3)_3COH_2^+ \ (m/z = 75) \longrightarrow (CH_3)_3C^{18}OH_2^+ \ (m/z = 77) + H_2O \quad (17)$$

$$H_2{}^{18}O + (CH_3)_3COH_2^+ \longrightarrow (H_2{}^{18}O)(H_2O)H^+ \ (m/z = 39) + (CH_3)_2CCH_2 \quad (18)$$

$$H_2{}^{18}O + (CH_3)_3COH_2^+ \longrightarrow (CH_3)_3C^+ \ (m/z = 57) + (H_2{}^{18}O)(H_2O) \quad (19)$$

according to reaction (18) has previously been observed by Hiraoka and Kebarle, and Hiraoka in high-pressure mass spectrometric experiments.[32, 33] Side reactions with background ammonia and *tert*-butanol, analogous to reactions (6) and (13)–(16), were also observed. The rate constants were determined to be $k_{17} = 4.0 \times 10^{-10}\ cm^3\,molecule^{-1}\,s^{-1}$ and $k_{19} = 6.4 \times 10^{-10}\ cm^3\,molecule^{-1}\,s^{-1}$, for reactions (17) and (19), respectively. The poor intensity of the protonated dimer peaks at $m/z = 39$ and $m/z = 41$, only allowed us to determine an upper limit for the rate constant for reaction 18, $k_{18} < 3 \times 10^{-11}\ cm^3\,molecule^{-1}\,s^{-1}$. Separate reactions showed that *tert*-butyl cations do not associate with water at any significant rate under the conditions used.

Ab initio models

Back-side nucleophilic displacement (S_N2_B): These identity gas-phase exchange reactions [Eq. (20)] were examined by

$$H_2O + ROH_2^+ \longrightarrow {}^+H_2OR + H_2O \quad (20)$$

quantum-chemical methods, partly to provide model potential energy profiles for the experiments, partly to study structural and energetic features of the reactions and partly to see how the results depend on the quantum-chemical method used. The latter point is of relevance in the last section in which we discuss the larger water clusters.

Computational costs for these large systems put a limit on the degree of sophistication with which they can be treated. It is therefore of great interest to see how the MP2//HF and HF wave functions perform relative to MP2 and B3LYP. The computational results for the potential-energy surfaces of the four (ROH_2^+, H_2O) systems are displayed in Figure 1 (geometries) and Figures 2–5 (potential energy diagrams). Two

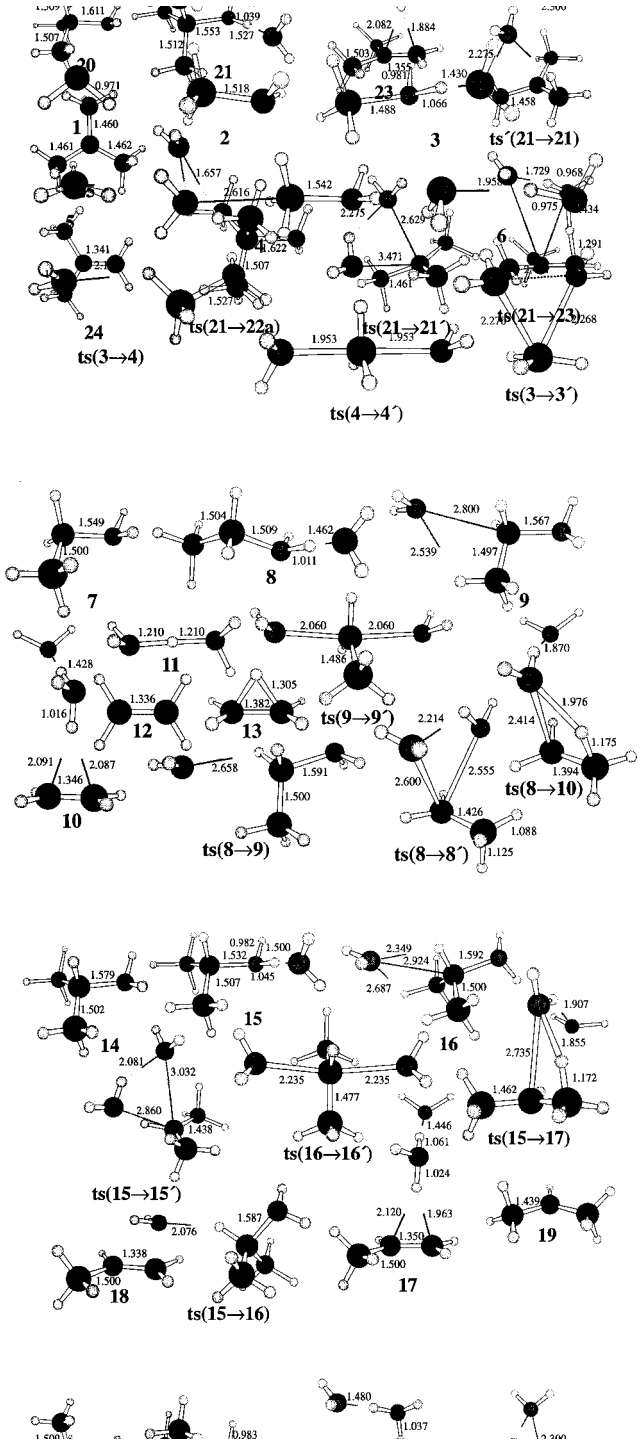

Figure 1. Structures of the stationary points obtained with MP2/6-31G(d). Bond lengths indicated are in Å. The cartesian coordinates for the structures referred to in this paper may be obtained from the authors upon request.

0947-6539/99/0506-1920 $ 17.50+.50/0 *Chem. Eur. J.* **1999**, *5*, No. 6

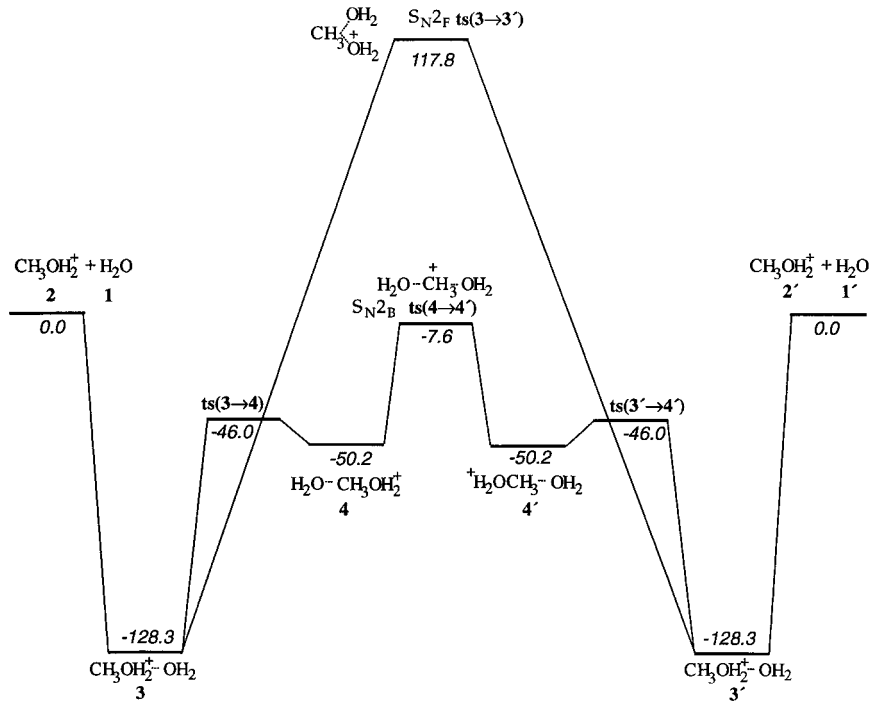

Figure 2. Potential energy diagram for the $[H_2O, CH_3OH_2]^+$ system from MP2/6-31G(d) calculations. Relative energies indicated are in kJ mol^{-1} and include zpve corrections.

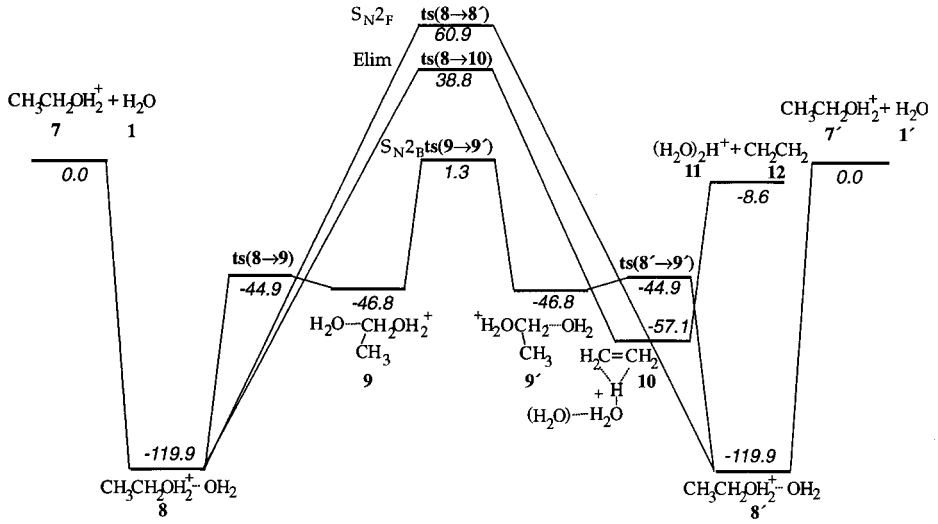

Figure 3. Potential energy diagram for the $[H_2O, CH_3CH_2OH_2]^+$ system from MP2/6-31G(d) calculations. Relative energies indicated are in kJ mol^{-1} and include zpve corrections.

different complexes may be formed upon association of a water molecule with a protonated alcohol according to Equations (21) and (22).

$$H_2O + ROH_2^+ \longrightarrow H_2O\cdots ROH_2^+ \quad \text{(C-side complex)} \qquad (21)$$

$$H_2O + ROH_2^+ \longrightarrow ROH_2^+\cdots OH_2 \quad \text{(O-side complex)} \qquad (22)$$

Our calculations show that in all cases both C-side and O-side complexes are stable molecular entities. However, the O-side complexes are of lower potential energy for all R groups (Figures 2–5). In all four systems the minimum energy path leads directly from the transition structure (**ts**) for S_N2_B to the C-side complex, so formally the C-side complex should be regarded as the direct precursor. We want to point out that isomerization between the C-side complex and the O-side complex is swift. In all cases the transition structure is only a few kJ mol^{-1} higher in potential energy than the corresponding C-side complex. This allows both potential-energy wells to be visited frequently before the transition state (TS) is traversed.

With all methods used (HF, MP2 and B3LYP) we were able to locate transition structures corresponding with an S_N2_B mechanism for all four systems, Figures 1–5 and Table 1. All methods give qualitatively similar results, with symmetrical transition-structure geometries in the sense that the O1–C and O2–C bond lengths (see Scheme 1 for definition of bond parameters) are the same to within 0.05 Å. The only exception is the HF transition structure for R = propyl which is clearly unsymmetrical, with d(O1–C) = 2.622 Å and d(O2–C) = 2.379 Å. However, the more complete MP2 and B3LYP methods give symmetrical structures as is evident from Table 1. Raghavachari et al. have performed HF/6-31G(d,p) calculations for the nucleophilic-substitution reactions between water and protonated methanol and ethanol.[34] Our TS geometries are similar to theirs.

The route to the S_N2_B transition structure is more cumbersome for the reaction between water and protonated *tert*-butanol than for the other systems. In this case an intermediate minimum, the inner-complex **22b**, was found between the initial C-complex, **22a**, and the transition structure, **ts(22→22′)**, with all the computational methods. The situation is shown in Figure 6. In the C-complex **22a**, all three methyl groups of the *tert*-butyl part interact in a largely noncovalent fashion with the oxygen of the incoming water molecule (O1). In order to obtain the inner-complex structure, one of the methyl groups rotates 60°; this permits a shorter contact distance between O1 and the central carbon atom (C). A

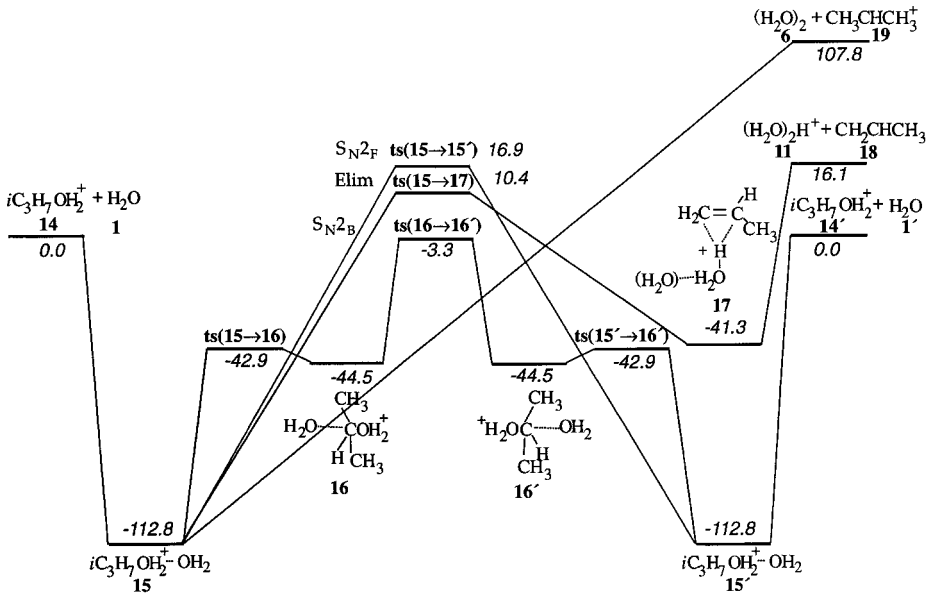

Figure 4. Potential energy diagram for the $[H_2O, (CH_3)_2CHOH_2]^+$ system from MP2/6-31G(d) calculations. Relative energies indicated are in kJ mol^{-1} and include zpve corrections.

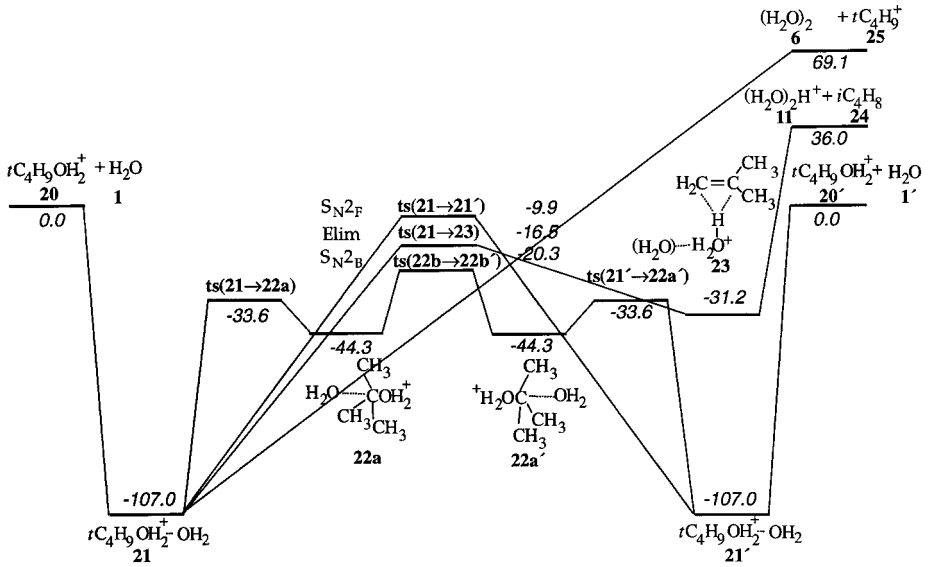

Figure 5. Potential energy diagram for the $[H_2O, (CH_3)_3COH_2]^+$ system from MP2/6-31G(d) calculations. Relative energies indicated are in kJ mol^{-1} and include zpve corrections.

substantial reduction in d(C–O1) and a corresponding increase in d(C–O2), the distance from the departing oxygen (O2), is observed. A transition structure, **ts(22a→22b)**, for the conversion of the C-complex to the inner-complex was located as shown in Figure 6. It is interesting to note that for passage from the inner-complex **22b** to its mirror-image structure **22b′** through **ts(22→22′)**, the actual substitution step requires rotation of a second methyl group coupled with a further shortening of the C–O1 bond. In fact, this coupling between rotation, bond shortening (C–O1) and bond lengthening (C–O2) is common for all substitution reactions, except for R = CH_3. However, for protonated *tert*-butanol we find that the methyl rotation is a more prominent part of the reaction coordinate at the TS than it is for the other systems.

The relevance of an inner-complex of the **22b** type can be sought in solution-phase chemistry. In their refinement of the original Ingold and Winstein mechanisms, Bentley, Schleyer and co-workers[9, 13] introduced the term intermediate S_N2 mechanism to explain how nucleophilic-substitution reactions of substrate molecules take place, which originally were believed to occur by means of the S_N1 mechanism. In their terminology, formation of a pre-transition-state intermediate is the key to the mechanism. The intermediate of their mechanism and the inner-complex found here appear to have the same characteristics.

The energy barrier $E_a = E_{ts} - E_{ccom}$ (energy of the TS minus energy of the C-complex) for the S_N2_B reaction follows the same trend with variation of the alkyl group for all the quantum-chemical methods employed, Table 1. Comparison of the HF and MP2 results is instructive. It is obvious that electron correlation is important for a reliable description of the energetics of the interaction during bond formation and fragmentation. Of particular importance is the finding that although the HF values appear to be quantitatively unreliable, the MP2//HF values are very close to the MP2 values. This is encouraging for the application of MP2//HF to larger systems (see section on clusters) where full MP2 treatment is prohibitive.

Although the barrier E_a is a key quantity for the reaction profile, the most relevant parameter for comparison with the ion-molecule experiments is the energy difference $\Delta E = E_{ts} - E_{react}$ (energy of the TS minus energy of the separated reactants). This figure follows the trend $(CH_3)_3C < CH_3 < (CH_3)_2CH < CH_3CH_2$ with variation of the alkyl group. Except for an interchange in the order between methyl and *iso*-propyl it resembles the trend found for the experimentally determined rate constants for substitution (see the previous section). In addition to ΔE, statistical factors affect the magnitude of the rate constants. These will be discussed in great detail in a later section.

It is enlightening to compare the interactions between the water molecules and the alkyl group in the transition structure

  0947-6539/99/0506-1922 $ 17.50+.50/0 *Chem. Eur. J.* **1999**, *5*, No. 6

Table 1. S_N2_B data.

	Method	CH_3-	CH_3CH_2-	$(CH_3)_2CH-$	$(CH_3)_3C-$
k, [$cm^3\,molecule^{-1}\,s^{-1}$]	experiment	2.2×10^{-13}	6.7×10^{-14}	4.6×10^{-11}	4.0×10^{-10}
E_a[a] [$kJ\,mol^{-1}$]	B3LYP	26.3	32.2	27.9	7.8
	MP2	42.6	48.1	41.3	23.8
	MP2//HF	44.7	50.1	41.8	23.8
	HF	30.5	22.4	4.3	−14.8
ΔE[b] [$kJ\,mol^{-1}$]	B3LYP	−23.0	−12.3	−14.5	−35.1
	MP2	−7.6	1.3	−3.3	−20.3
	MP2//HF	−5.3	3.6	−2.3	−18.6
	HF	−14.4	−18.6	−33.4	−52.4
r_1 [Å][c]	B3LYP	1.553	1.590	1.642	1.724
	MP2	1.542	1.565	1.592	1.627
	HF	1.538	1.572	1.617	1.742
r_2 [Å][c]	B3LYP	2.597	2.818	3.413	3.392
	MP2	2.616	2.811	2.924	3.419
	HF	2.690	2.874	3.020	3.487
r_3 [Å][c]	B3LYP	1.974	2.083	2.261	2.787
	MP2	1.953	2.060	2.235	2.689
	HF	2.039	2.209	2.622	2.787
r_4 [Å][c]	B3LYP	1.974	2.104	2.261	2.830
	MP2	1.953	2.060	2.235	2.726
	HF	2.039	2.209	2.622	2.814
$\tilde{\nu}_{ts}$[d] [cm^{-1}]	B3LYP	**i**·363[e]	**i**·311[e]	**i**·261[e]	**i**·156[f]
	MP2	**i**·499[e]	**i**·428[e]	**i**·296[e]	**i**·166[f]
	HF	**i**·369[e]	**i**·199[f]	**i**·117[f]	**i**·135[f]

[a] Activation energy; energy of the transition structure minus energy of the C-complex. [b] Energy difference; energy of the transition structure minus energy of the reactants. [c] See Scheme 1 for definition. [d] Imaginarg frequency. [e] The reaction coordinate is dominated by the O1···C···O2 asymmetric stretching motion. [f] The reaction coordinate is a hybrid of the O1···C···O2 asymmetric stretching motion and rotation of one of the methyl groups.

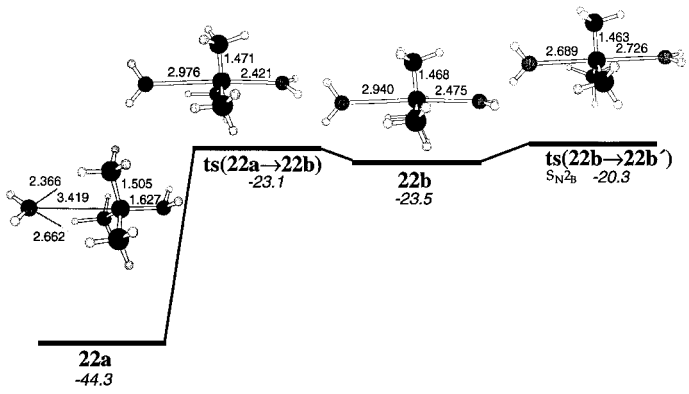

Figure 6. Partial potential energy diagram for the S_N2 reaction between H_2O and $(CH_3)_3COH_2$. Relative MP2/6-31g(d) energies indicated are in $kJ\,mol^{-1}$ and include zpve corrections. Bond lengths indicated are in Å.

$(H_2O\cdots R^+\cdots OH_2)$ with those in the reactants ($ROH_2^+ + H_2O$) and the completely separated sub-units ($R^+ + H_2O + H_2O$). The dissociation energy of the C–O bond (E_{C-O}) in ROH_2^+ to give $R^+ + H_2O$ decreases monotonically with the number of methyl groups attached to the central carbon atom. We notice that our MP2 and B3LYP calculations overestimate this bond energy by on average 25 $kJ\,mol^{-1}$ and 29 $kJ\,mol^{-1}$, respectively, compared with reliable experimental data, Figure 7.

It is well-known that substituent alkyl groups stabilize carbocations.[14] In accordance with common practice we

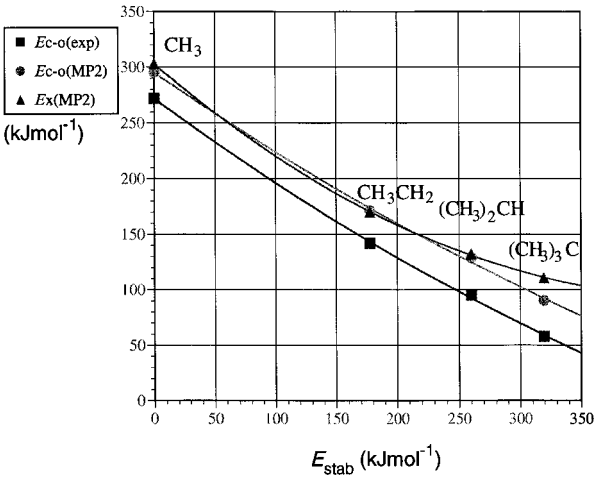

Figure 7. Plot which shows the variation in the bond strengths of the transition state (E_x) and the protonated alcohol (E_{C-O}) as a function of the stabilization energy (E_{stab}) for the individual systems. The energy quantities are defined in the text.

define the stabilization energy E_{stab} for each of the carbocations relevant to this study in terms of the enthalpy change for the isodesmic reaction given in Equation (23), in which $n=0$, 1, 2 and 3 for CH_3, CH_3CH_2, $(CH_3)_2CH$ and $(CH_3)_3C$, respectively.

$$(CH_3)_nCH_{3-n}^+ + H{-}CH_3 \longrightarrow CH_3^+ + (CH_3)_nCH_{4-n} \quad (23)$$

Experimentally determined heats of formation were used.[35, 36] When E_{C-O} is plotted against E_{stab} (Figure 7), it turns out that the ability of the carbocation to bind water decreases with increased stabilization. In other words, the electrophilicity of the central carbon decreases with increased methyl substitution because the positive charge is dispersed to the periphery. The same trend is found for the dissociation of the TS into its three component parts [Eq. (24)].

$$(H_2O\cdots R^+\cdots OH_2) \longrightarrow R^+ + H_2O + H_2O \quad (24)$$

The corresponding dissociation energy E_x for a given R group is close to the C–O bond-dissociation energy of the protonated alcohol E_{C-O} (Figure 7). This means that the interactions between the two water molecules and the central carbocationic unit of the transition structures are influenced by the same methyl-group stabilization, and correspondingly the E_x values, decrease in the order: $CH_3 > CH_3CH_2 > (CH_3)_2CH > (CH_3)_3C$. The same trend is found when we compare the variation of the C–O bond lengths in the protonated alcohols and in the transition structures (Figure 1). In the TS for the reaction between water and protonated *tert*-butanol [**ts(22→22′)**, Figure 6] the central *tert*-butyl moiety bears a strong structural resemblance to the free *tert*-butyl cation **25**. The interaction between the central alkyl moiety and the two water molecules is mainly through electrostatics and polarization. Although the structure is labile and the mechanism is formally S_N2, not S_N1, it is perfectly justifiable to term this a solvated carbocation. As we gradually move to the transition structures for substitution of

the less methyl-substituted species ($R = (CH_3)_2CH$, CH_3CH_2, CH_3), it is clear that the interactions in the transition structures become increasingly covalent.

It is well-known from solution studies that the rates of S_N2 reactions decrease with increasing methyl-group substitution on the α carbon (i.e., $CH_3 > CH_3CH_2 > (CH_3)_2CH > (CH_3)_3C$). A few examples are known from the gas phase in which the same reactivity trend is found, for example, in reactions of the type exemplified by Equation (25), in which X^- and Y^- are halide anions.[37–40]

$$X^- + RY \longrightarrow Y^- + RX \quad (25)$$

A number of different explanations have been put forward to explain this trend.[2, 12, 41–45] All these are based on assumptions regarding the intrinsic properties of the molecules. Most of them focus on the interactions between the methyl group(s) and the carbocationic centre, the nonbonding interaction between the nucleophile and the leaving group, and their interactions with the methyl groups. The term steric hindrance is often adopted to describe this phenomenon. It is very interesting that steric hindrance appears not to be a factor for gas-phase reactions between water and protonated alcohols, and for this reason it is not a universal phenomenon in S_N2 reactions. Water is quite a poor nucleophile and its ability to donate electrons to a carbocationic centre is therefore more limited than for example a halide ion. For this reason the electron-donating ability of the methyl group will be more pronounced in the case of a poor nucleophile/nucleofuge. Based on this finding we would recommend that the term steric hindrance should be more precisely defined in use (e.g., limited to purely entropic effects).

The reactivity trend we have found has some precedence in work on reactions between alcohols and protonated alcohols, and between formaldehyde and protonated alcohols.[46–50] In the explanation of Karpas and Meot-Ner[50]—based on an empirical linear relationship between reaction rate and some of the $R{-}OH_2^+$ dissociation energies—they infer a steric hindrance, which appears to be partly enthalpic and partly entropic in origin. We do, however, admit that we have difficulty in understanding their interpretation completely.

In a later section we present results from cluster models for the reactions which show that in solution the reactivity trend of protonated alcohols is the same as that of the halides.

Front-side nucleophilic displacement (S_N2_F): Besides the traditional back-side displacement mechanism (S_N2_B) there is, at least in principle, a possibility that the nucleophile attacks from the same side as the leaving group departs in the reaction depicted in Equation (26).

$$H_2O + ROH_2^+ \longrightarrow {}^+H_2OR + H_2O \quad (26)$$

While back-side displacement gives inversion of configuration at the central carbon atom of the substrate molecule, front-side displacement (S_N2_F) results in retention of configuration. The possibility of front-side attack was originally considered in connection with mechanistic investigations of the reaction between methanol and protonated methanol. This reaction eliminates water with consequent formation of protonated dimethyl ether [Eq. (5)].[51–53] It was, however, concluded that in this instance the S_N2_F mechanism is not of significance. This was also the conclusion from a study of the homologous gas-phase reaction in the *s*-butanol system.[54, 55] Despite these few negative results, the S_N2_F mechanism is of fundamental interest because it may explain why so many solvolysis substitution reactions occur with partial retention of configuration.[6] We have attempted to answer this question by a systematic search for transition structures in which the two water entities exchange on the same side of the substrate in reactions between water and protonated alcohols.

The results are presented in Figures 1–5. In all cases the O-complex is the formal precursor for the S_N2_F transition structure. It is clear that front-side displacement via **ts(3→3′)** is unimportant in the substitution of water in protonated methanol because it is 110 kJ mol^{-1} higher in potential energy than **ts(4→4′)**. Although the potential energy of the transition structure for S_N2_F lies above that for S_N2_B for $R = CH_3$ [**ts(3→3′)**], CH_3CH_2 [**ts(8→8′)**], $(CH_3)_2CH$ [**ts(15→15′)**] and $(CH_3)_3C$ [**ts(21→21′)**], the difference becomes gradually smaller when the number of methyl substituents increases. For $R = (CH_3)_3C$ the difference between the S_N2_F and S_N2_B transition structures is only 10 kJ mol^{-1}, so it is quite likely that front-side substitution may contribute somewhat to the overall substitution observed in the experiment. It may also play a minor role for $R = (CH_3)_2CH$.

For $R = (CH_3)_3C$ we observe that the transition structure **ts(21→21′)** has a distinct carbocationic character; this indicates that this species is a *tert*-butyl cation solvated by a water dimer. The interaction is noncovalent, as is evident from the structural parameters in Figure 1. One should notice the structural resemblance between this species and the species discussed in connection with the S_N2_B mechanism [**22b**, **ts(22a→22b)** and **ts(22b→22b′)**].

Computational data from Berthomieu and Audier have established that protonated *tert*-butanol has a loosely bonded isomer $C_4H_9^+ \cdots OH_2$ (a potential-energy minimum) in addition to the covalent isomer $C_4H_9OH_2^+$.[56] In the $C_4H_9^+ \cdots OH_2$ complex the water oxygen is in close contact with one hydrogen from each of two of the methyl groups. The water molecule lies in the mirror plane bisecting the central carbon and the third methyl group.

Numerous attempts to locate an energy minimum corresponding with an analogous weakly bonded species $C_4H_9^+ \cdots (OH_2)_2$ failed and lead without exception to $C_4H_9OH_2^+ \cdots (OH_2)$ (**21**) upon geometry optimization. Likewise, no minimum corresponding with $C_3H_7^+ \cdots (OH_2)_2$ was found, although we were able to locate a minimum for $C_3H_7^+ \cdots (OH_2)$ with MP2. On the other hand, we note the close similarity between the complex of Berthomieu and Audier, $C_4H_9^+ \cdots OH_2$, and the species $H_2O \cdots C_4H_9^+ \cdots OH_2$ (**22b**), the intermediate inner-complex of the S_N2_B mechanism. Except for the extra water molecule with a C–O length of 2.475 Å and close contact with one hydrogen of the third methyl group, they are practically identical (Figure 6). During the search for the proper TS for water exchange **ts(21→21′)**, an additional stationary structure **ts′(21→21′)**, formally a

0947-6539/99/0506-1924 $ 17.50+.50/0 *Chem. Eur. J.* **1999**, *5*, No. 6

transition structure with an imaginary frequency of vibration of only 15**i** cm^{-1}, was located and is very close to **ts(21 →21′)** in energy. This species has all the characteristics of a complex of the type $C_4H_9^+ \cdots (OH_2)_2$, except that it is not a minimum. Moreover, it is also distinct from **ts(21 →21′)** in the sense that it does not lead to exchange of the two water moieties.

From this discussion we must conclude that there are no stable $R^+ \cdots (OH_2)_2$ species for any of the potential-energy surfaces investigated. This may cast some doubt on the hypothesis that absolutely free carbocations exist in solution because addition of further water molecules would probably not give rise to $R^+ \cdots (OH_2)_n$ ($n = 3, 4,\ldots$), since water clusters with three or more water molecules have higher proton affinities than the corresponding alkenes, R–H (vide infra). On the other hand, the existence of $H_2O \cdots C_4H_9^+ \cdots OH_2$ (**22b**) would indicate that similar structures could be present in solution.

The topography of the $[C_4H_9, (OH_2)_2]^+$ potential-energy surface poses a challenge when one wants to extract the formal nature of the reactions that one observes. The surface is extremely flat, and the calculated curvature in the region in which the substitutions take place may have errors owing to the incomplete wave functions. A discussion of the substitution mechanisms that is based only on the topography of the potential-energy surface is in any event too limited. The detailed dynamics of a system that possesses sufficient energy to react has to be taken into account. The flatness of the potential-energy surface allows numerous reaction trajectories to trace out configurations of the type $C_4H_9^+ \cdots (OH_2)_2$ and $H_2O \cdots C_4H_9^+ \cdots OH_2$. By doing so the system spends a considerable time with a structure which for all practical purposes must be regarded as a solvated carbocation, even though some of these transient structures do not represent local minima.

One more alternative for front-side substitution may be available if the elimination reaction is reversible, [Eq. (27)] and the $CH_3CR_2OH_2^+ \cdots OH_2$ complex dissociates after the two water molecules have exchanged within the $(CH_2CR_2) \cdots (H_3O^+)(H_2O)$ complex. This possibility was investigated further, and will be discussed in the context of the elimination reactions in the next section.

$$CH_3CR_2OH_2^+ \cdots OH_2 \rightleftharpoons (CH_2CR_2) \cdots (H_3O^+)(H_2O) \quad (27)$$

Elimination (E2): It has been observed that the proton affinity of a water cluster, $(H_2O)_n$, generally increases with its size. The proton affinities (PA) of some small clusters are, in kJ mol^{-1} (figures in brackets are the literature experimental value[35, 57] and our calculated MP2 value): H_2O (691, 704); $(H_2O)_2$ (806, 839); $(H_2O)_3$ (871, 888). The proton affinity of bulk water is 1130 kJ mol^{-1}.[58] As we see, the MP2 calculations slightly overestimate these PAs. The proton affinities for the alkenes relevant to this study are: CH_2CH_2 (681, 681); CH_3CHCH_2 (752, 748); $(CH_3)_2CCH_2$ (796, 806). In order for alkene formation to take place upon reaction between water and a protonated alcohol [Eq. (28)] the overall reaction must

$$H_2O + ROH_2^+ \longrightarrow (R{-}H) + (H_2O)_2H^+ \quad (28)$$

be exothermic, or only slightly endothermic. As a part of this requirement the proton affinity of the water dimer must be larger than the proton affinity of the alkene, R–H. From the data above we see that this is the case for all systems, except for the reaction between water and protonated methanol. Although elimination of water is possible from protonated methanol—a process which gives singlet methylene[59]—it requires considerable energy and will therefore not be discussed further.

As is evident from Figure 3, ethylene formation in the reaction between water and protonated ethanol is thermodynamically favourable [Eq. (8)]. The computed heat of reaction is in good agreement with available thermochemical data from the literature. The reason why the reaction is so slow compared with the substitution reaction is the unfavourably high barrier. The transition structure **ts(8 →10)** is shown in Figure 1. The key step is transfer of a proton from the alkyl group to the oxygen that originally belonged to the alcohol. The incoming water molecule is a spectator and acts as a solvent in this transition structure. Elimination of water from protonated ethanol [Eq. (29)] has been studied theoretically

$$CH_3CH_2OH_2^+ \longrightarrow CH_2CH_2 + H_3O^+ \quad (29)$$

by Bouchoux and Hoppiliard,[60] and by Swanton, Marsden and Radom[61] with only slightly different computational methods from those used here. The transition structures found by these workers are very similar to **ts(8 →10)**, except for the extra water molecule. Comparison between our data and the data reported for the reaction in Equation (29) reveals that the presence of the extra water molecule increases the barrier substantially. In other words, the transition structure is less stabilized by solvation than the reactants.

For the reaction between water and protonated *iso*-propanol, the thermochemistry for propene formation is less favourable, although the reaction is only slightly endothermic in this case. On the other hand the barrier is lower, so the reaction is observed in the experiment. Because the proton transfer is also the rate-determining step in this case, it is very likely that the effective barrier is lower than the calculated relative potential energy of **ts(15 →17)** owing to the effect of quantum-mechanical tunnelling.[62]

Isobutene formation from water and protonated *tert*-butanol is more endothermic (experimental value is 28 kJ mol^{-1}, MP2 value is 36 kJ mol^{-1}), but the calculated barrier is lower than for *iso*-propanol. The alternative elimination pathway, loss of the water dimer with formation of $(CH_3)_3C^+$, is even more endothermic (experimental value is 38 kJ mol^{-1}, MP2 value is 69 kJ mol^{-1}). Despite this the latter elimination pathway dominates. This must be due to the fact that butene formation requires passage through the tight transition state for the proton transfer, while butyl cation formation results from direct bond cleavage. The formation of the *tert*-butyl cation in this reaction may be regarded as a gas-phase analogue of the first stage of an E1 mechanism. One should also note that in the reaction between water and protonated *iso*-propanol, some *iso*-propyl cation formation was observed.

At a temperature of 0 K we would not expect to observe the slightly endothermic elimination reactions described here. The observation of the apparently endothermic processes in the reaction between water and protonated *tert*-butanol (and also in the reaction of water and protonated *iso*-propanol) is therefore interesting. The straight lines obtained in the semi-logarithmic plots of the normalized intensity of the reactant ion makes us confident that the reactant ions are not superthermal (see the Experimental Section). Although vibrational excitation is rather modest at 300 K, there is nevertheless some internal energy available. The internal energy increases with the size of the system, and the average energies (of the reactant systems $H_2O + ROH_2^+$ based on the rigid rotor–harmonic oscillator approximation with the molecular parameters from the MP2 calculations) are 9.3 kJ mol^{-1} (methyl), 11.9 kJ mol^{-1} (ethyl), 14.4 kJ mol^{-1} (*iso*-propyl), and 18.5 kJ mol^{-1} (*tert*-butyl). Our statistical mechanical treatment of all internal degrees of freedom as harmonic oscillators is obviously a coarse simplification. Because protonated *tert*-butanol has several internal modes, which at room temperature are effectively free rotations rather than vibrations, the value given here is certainly an underestimate. Also by taking the uncertainty of the experimental heats of formation of the species involved into account, we find that the reactions are very likely to be energetically allowed. On an average this thermal energy (as computed from the MP2 heat capacities) is sufficient for the reactions to take place. This will be discussed further in the next section.

For the system with $R = CH_3CH_2$ a transition structure, **ts(10→10′)**, of C_2 symmetry with a potential energy of -38.2 kJ mol^{-1} relative to the reactants (on the energy scale used in Figure 3) was located. The reaction coordinate of **ts(10→10′)** in Figure 8 is a hybrid of two motions; proton

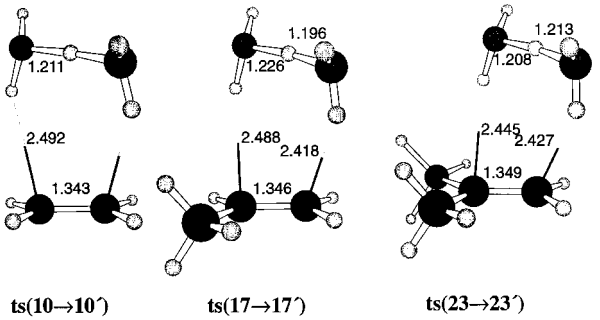

Figure 8. Structures of the transition states for exchange of the two water molecules within each of the elimination-product complexes (MP2/6-31G(d)). Bond lengths indicated are in Å. These transition structures provide an alternative mechanism for substitution with retention of configuration as explained in the text.

transfer within the $(H_2O)_2H^+$ moiety and exchange of the positions of the two water molecules. This TS is lower in energy than the products, CH_2CH_2 (**12**) and $(H_2O)_2H^+$ (**11**), and may in principle allow the two water molecules to interchange before completion of the elimination pathway, or before an alternative course of events in which one water molecule is lost. In the latter case the net outcome is substitution if the so-formed $[CH_2CH_2]\cdots[H_3O^+]$ species isomerizes to protonated ethanol. Upon closer inspection it turns out that this gives rise to a substitution reaction with retention of configuration at the carbon centre. It is difficult to judge the importance of this hidden pathway for substitution in our experiments. In order to do so, very extensive reaction dynamics simulations would be needed.

For $R = (CH_3)_2CH^+$ and $(CH_3)_3C^+$ similar transition structures were found. They are displayed in Figure 8. The potential energy of **ts(17→17′)** is -20.7 kJ mol^{-1} relative to the reactants on the energy scale used in Figure 4. The corresponding value for **ts(23→23′)** is -7.9 kJ mol^{-1} (Figure 5). We can therefore conclude that the hidden pathways for substitution are also energetically accessible for the *iso*-propyl and *tert*-butyl systems.

RRKM calculations. Estimation of barriers for S_N2_B: We have used microcanonical variational transition-state theory to estimate the rates of the S_N2_B reactions as a function of their barriers in the form of the energy difference $\Delta E = E_{ts} - E_{react}$ (energy of the TS minus energy of the separate reactants). The method, successfully used by Brauman and co-workers for the S_N2 reaction [Eq. (30)] was followed step-by-step.[31] The reaction scheme given in Equation (31) was employed.

$$^{35}ClCH_2CN + {}^{37}Cl^- \longrightarrow {}^{35}Cl^- + {}^{37}ClCH_2CN \quad (30)$$

$$H_2O + ROH_2^+ \underset{k_{-c}}{\overset{k_c}{\rightleftharpoons}} ROH_2^+\cdots OH_2 \xrightarrow{k_p} \text{products} \quad (31)$$

Before proceeding with the discussion of the microcanonical variational theory calculations, we need to consider the bond strengths in the important intermediates $ROH_2^+\cdots OH_2$ more closely. The bond-dissociation energies of the hydrogen-bonded O-complexes (E_{ocom}) are defined according to Equation (32). A plot of E_{ocom} obtained with the various computa-

$$ROH_2^+\cdots OH_2 \longrightarrow ROH_2^+ + H_2O \qquad (E_{ocom}) \quad (32)$$

tional methods against the experimental difference in proton affinities[36] of the alcohols (ΔPA; Figure 9) gave very good linear relationships.[63, 64] The plots also include water (R = H). While the experimental E_{ocom} values[57, 63] for protonated water, methanol and ethanol fall nicely on a straight line, the corresponding values for protonated *iso*-propanol and *tert*-butanol deviate considerably. Although we cannot absolutely rule out systematic errors in the calculations, it is reasonable to assume that the deviations are due to imperfect experimental data for R = *i*Pr and *t*Bu. We therefore believe that more reliable estimates for the hydrogen-bond strengths are obtained by extrapolation of the linear part of the line as indicated in Figure 9.

To calculate the overall reaction rates we made the following assumptions:

1) The rate of isomerisation between the C-complex and the O-complex was assumed to be much faster than k_p and k_{-c}.
2) The equilibrium constant $K = k_c/k_{-c}$ was calculated from the partition functions for the two systems $H_2O + ROH_2^+$ and $ROH_2^+\cdots OH_2$.

0947-6539/99/0506-1926 $ 17.50+.50/0 *Chem. Eur. J.* **1999**, *5*, No. 6

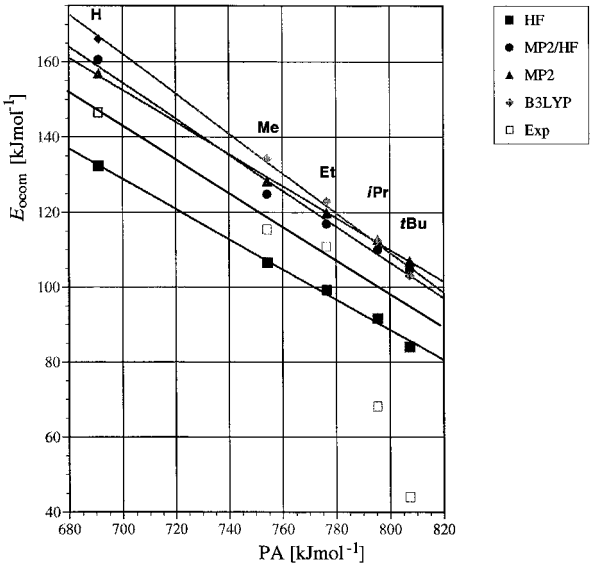

Figure 9. Correlation between hydrogen-bond strengths (E_{ocom}) in the O-complexes, $ROH_2^+ \cdots OH_2$, and the proton affinities (PA) of the alcohols ROH. The theoretical E_{ocom} numbers refer to energies, while the experimental data are based on relative enthalpies of formation.

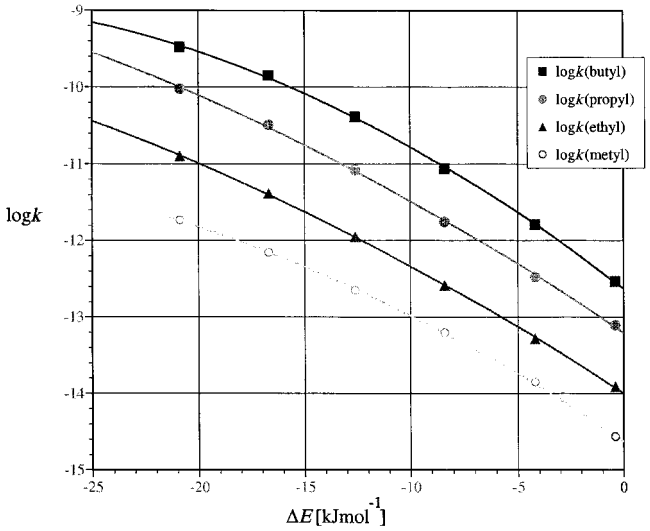

Figure 10. Relationship between log k, the logarithm of the overall bimolecular rate constant, and ΔE, the difference between the energy of the transition structure $[H_2O \cdots R \cdots OH_2]^+$ and the reactants, $H_2O + ROH_2^+$. The data are obtained from variational transition-state theory calculations as explained in the text.

3) Once formed, the intermediate $ROH_2^+ \cdots OH_2$ either dissociates to regenerate the reactants or reacts through the transition structure for S_N2_B.
4) The angular momentum distribution $P(J)$ was calculated according to the original scheme of Waage and Rabinovitz.[65]
5) Internal degrees of freedom were either considered to be harmonic vibrations or rigid internal rotations. Harmonic frequencies (scaled) and moments of inertia were taken from the MP2-optimized structures of the species involved.
6) The interaction potential, $V(r^*)$, of the protonated alcohol and water, along the reaction coordinate r^* for back dissociation was modelled with the equilibrium geometries of the two species, the known or extrapolated experimental bond-dissociation energies Figure 9 and the experimental dipole moment and polarizability of water.

The variational RRKM calculations were performed with the procedures of the program HYDRA. The models were shown to be robust in the sense that variations in bond-dissociation energies, harmonic frequencies and moments of inertia only affect the rate constants slightly. The only parameter which significantly influences the rate constants is the sought ΔE.

The results are presented in Figure 10 and show how the rate constants vary with the ΔE values. The rates for substitution in protonated methanol and protonated ethanol were experimentally determined to be $k_4 = 2.2 \times 10^{-14}$ cm^{3}molecule^{-1}s^{-1} and $k_7 = 6.7 \times 10^{-14}$ cm^{3}molecule^{-1}s^{-1}, respectively (see first section under Results and Discussion). In these two cases there is no competing elimination reaction, and we obtain ΔE values of -13 kJmol^{-1} and -5 kJmol^{-1}. The corresponding MP2 values are -8 kJmol^{-1} and $+1$ kJmol^{-1}, and the ab initio model and the variational RRKM analysis are therefore seen to be in good agreement.

For protonated *iso*-propanol and *tert*-butanol the situation is complicated by the occurrence of the competing elimination reactions. We decided only to model the substitution for two reasons. First, the elimination reaction is a process that involves quantum-mechanical tunnelling through the potential energy barrier. In principle this could be explicitly taken into account in the rate-constant calculation, but not without introducing additional and uncertain approximations. Second, and more important is the fact that in these two cases we would have to determine three or four different ΔE values based on only two known rate constants. The problem is that we do not know the separate rate constants for the S_N2_B and S_N2_F processes from the experiments, only their sum. In addition to this we do not know to what extent the hidden substitution mechanism is operative as already discussed in earlier sections. We shall therefore limit ourselves to a qualitative determination of the ΔE values for R = *iso*-propyl and *tert*-butyl as if elimination did not occur. The raw ΔE values obtained from Figure 10, with the experimental substitution rates of $k_{10} = 4.6 \times 10^{-11}$ cm^{3}molecule^{-1}s^{-1} and $k_{16} = 4.0 \times 10^{-10}$ cm^{3}molecule^{-1}s^{-1} are -18 and -23 kJmol^{-1}. The corresponding MP2 values for the S_N2_B reaction are -3 and -20 kJmol^{-1}; this is at least in qualitative agreement.

At this stage of the discussion we are in the position to evaluate the performance of the different quantum-chemical methods. The conclusion to be drawn from the quite detailed statistical analysis in this section is that the MP2 model appears to be nearly quantitatively correct, at least for those systems that are accessible for full testing (R = CH_3 and CH_3CH_2). It is also evident as indicated in the previous sections, that the MP2 calculations reproduce the observed reactivity very well. In the case of the *iso*-propyl system it appears that the MP2 barrier for S_N2_B is slightly too high. The B3LYP, HF and MP2//HF results confirm the MP2 model in the sense that all general trends—relative barrier heights for S_N2_B, E2 and S_N2_F and the pattern in reactivity between the

four systems—are the same. The HF model gives unsatisfactory results for the absolute barrier heights, and the agreement with experimentally known relative energies turns out to be less good than for the other methods. Despite this, the MP2//HF and MP2 results are identical to within a few kJ mol^{-1}. The B3LYP results are quite close to the MP2 results with regard to barrier heights. In some cases the agreement with experimentally known relative energies is worse, and in some cases it is better.

Hydrolysis of larger clusters. Correspondence with solution: Ab initio calculations of solvent effects may be performed with two approaches quite different in principle,[19, 66] the super-molecule approach or the reaction-field approach. In the super-molecule model, a limited number of solvent molecules are included together with the reacting unit, and the combined system is treated homogeneously. In the reaction-field model the reacting unit is embedded in a dielectric continuum, and the interaction between the solvent molecules and the reacting unit is treated by means of perturbation theory. The two methods may also be combined. Both approaches have their advantages, but we chose to apply the super-molecule approach in this case because this gave us a chance to study the effects of successive addition of water molecules.

We have limited the treatment to the S_N2_B and the elimination mechanisms. The cluster or microsolvation reactions in Equations (33) – (35) were studied.

$$H_2O[H_2{}^*O\cdots R{-}OH_2{}^+]OH_2 \longrightarrow H_2O[{}^+H_2{}^*O{-}R\cdots OH_2]OH_2 \quad (33)$$

$$(H_2O)_2[H_2{}^*O\cdots R{-}OH_2{}^+](OH_2)_2 \longrightarrow (H_2O)_2[{}^+H_2{}^*O{-}R\cdots OH_2](OH_2)_2 \quad (34)$$

$$(H_2O)_2[H_2{}^*O\cdots R{-}OH_2{}^+](OH_2)_2 \longrightarrow (H_2O)_2[H_2{}^*O\cdots (R{-}H)\cdots H_3O^+](OH_2)_2 \quad (35)$$

The reaction in Equation (33), the small model with two extra water molecules, was studied only for $R = CH_3$, the reaction in Equation (34), the large model with two extra water molecules, was studied for all systems, and the reaction in Equation (35), the large model with four extra water molecules, was studied for all systems except $R = CH_3$. Owing to the size of the systems, geometries were optimized with HF, whilst energies were computed with MP2. As already mentioned the performance of this MP2//HF method was demonstrated to be satisfactory for the unsolvated systems in the sense that the energies are almost identical to those obtained from the pure MP2 method.

To deal with the effects of solvation, we introduce the following definitions for the energies of solvation (E_{sol}) for the separate reactants [r; Eq. (36)], the actual reactant configuration [intermediate; i; Eq. (37)], the TS for for S_N2_B [tssn; Eq. (38)] and the TS for E2 [tsel; Eq. (39)] (in the case of the small model, the four waters are replaced by two).

$$H_2O + R{-}OH_2{}^+ + 4H_2O \longrightarrow (H_2O)_3 + R{-}OH_2{}^+(OH_2)_2 \quad -E_{sol,r} \quad (36)$$

$$[H_2O\cdots R{-}OH_2{}^+] + 4H_2O \longrightarrow (H_2O)_2[H_2O\cdots R{-}OH_2{}^+](OH_2)_2 \quad -E_{sol,i} \quad (37)$$

$$[H_2O\cdots R^+\cdots OH_2] + 4H_2O \longrightarrow (H_2O)_2[H_2O\cdots R^+\cdots OH_2](OH_2)_2 \quad -E_{sol,tssn} \quad (38)$$

$$[(R{-}H)\cdots H^+\cdots OH_2\cdots (OH_2)] + 4H_2O \longrightarrow (H_2O)_3[(R{-}H)\cdots H^+\cdots OH_2\cdots (OH_2)](OH_2) \quad -E_{sol,tsel} \quad (39)$$

The most relevant energy data are presented in Tables 2 and 3. Figure 11 shows the reactants and transition states for the reactions given in Equation (33) [upper panel] and Equation (34) [lower panel] for the case where $R = CH_3$. While the gas-phase reactivity is largely determined by the difference $\Delta E = E_{ts} - E_{react}$ the parameter of interest for a reaction in solution is $E_{a,sol} = E_{ts} - E_{ccom} - (E_{sol,ts} - E_{sol,i})$, that is, the energy of the solvated TS minus the energy of the solvated C-complex {reactant configuration; $(H_2O)_2[H_2O\cdots R{-}OH_2{}^+](OH_2)_2$}. In the case of the S_N2_B reaction, it turns out

Table 2. Solvation effects for S_N2_B (MP2//HF), energies in kJ mol^{-1}, distances in Å.

	Small CH_3-	Large CH_3-	Large CH_3CH_2-	Large $(CH_3)_2CH-$	Large $(CH_3)_3C-$
$E_r - E_{ccom}$	50.0	50.0	46.5	43.9	42.5
ΔE	− 5.3	− 5.3	3.6	2.0	18.6
E_a	44.7	44.7	50.1	41.9	23.8
$-E_{sol,r}$	146.5	297.5	285.2	275.3	267.3
$-E_{sol,i}$	155.9	277.0	268.2	262.6	255.6
$-E_{sol,tssn}$	139.6	252.3	234.9	209.9	182.6
$E_{a,sol}$	61.0	69.4	83.4	94.6	96.8
r_1(free/sol)	1.538/1.504	1.538/1.485	1.572/1.501	1.617/1.523	1.742/1.546
r_2(free/sol)	2.690/2.686	2.690/2.711	2.874/2.871	3.020/3.023	3.487/3.498
r_3(free/sol)	2.039/2.008	2.039/1.983	2.209/2.083	2.379/2.245	2.814/2.560
r_4(free/sol)	2.039/2.008	2.039/1.983	2.209/2.092	2.622/2.250	2.787/2.628

Table 3. Solvation effects for elimination (MP2//HF), energies in kJ mol^{-1}.

	Large CH_3CH_2-	Large $(CH_3)_2CH-$	Large $(CH_3)_3C-$
$E_r - E_{ccom}$	46.5	43.9	42.5
ΔE	31.9	21.6	− 23.7
E_a	78.4	65.5	18.8
$-E_{sol,r}$	285.2	275.3	267.3
$-E_{sol,i}$	268.2	262.6	255.6
$-E_{sol,tsel}$	218.0	209.9	167.4
$E_{a,sol}$	128.5	118.3	106.2

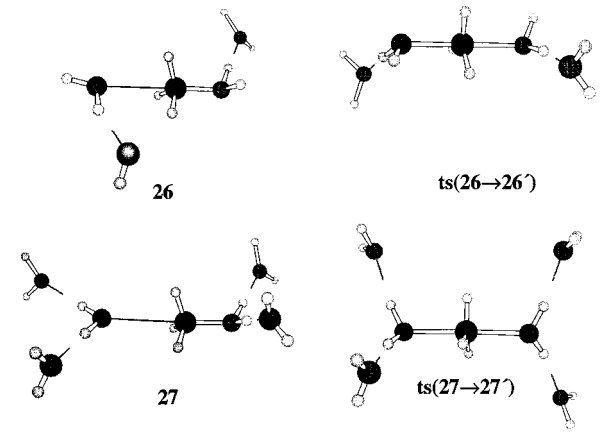

Figure 11. HF/6-31g(d) structures for the small (upper) and large (lower) clusters simulating nucleophilic substitution for $[H_2O, CH_3OH_2]^+$ in water. Reactant configurations are shown on the left and the transition structures are shown on the right.

0947-6539/99/0506-1928 $ 17.50+.50/0 *Chem. Eur. J.* **1999**, *5*, No. 6

that without exception the transition structures are less strongly solvated than the reactant configurations, that is, $E_{sol,tssn} < E_{sol,i}$. Furthermore, this tendency increases with addition of water molecules, (large model vs. small model). This is not unexpected because the interactions between the surrounding water molecules and the reacting unit is through hydrogen bonds, and a protonated alcohol forms much stronger hydrogen bonds than the more or less free incoming and outgoing water molecules of the transition structures. This may be deduced from the interatomic distances (not shown here). A simple electrostatic analysis leads to the same conclusion because the transition structures for the S_N2_B reaction are all symmetrical, while the reacting protonated alcohols possess quite substantial dipole moments and are therefore subject to a greater energy lowering from perturbation of the surrounding dielectric medium.

The difference in solvation energies between TS and reactant decreases in the order: $(CH_3)_3C > (CH_3)_2CH > CH_3CH_2 > CH_3$. By combining the solvation energy difference with the intrinsic energy barrier calculated (vide supra), we find that the barriers for the cluster model of the S_N2_B reaction decrease in the order: $(CH_3)_3C > (CH_3)_2CH > CH_3CH_2 > CH_3$. Unfortunately, we have not been able to find comparable experimental reactivity data in the literature in which the alkyl groups have been systematically varied in order to probe S_N2 water substitution in protonated alcohols. We do, however, see that the trend is the same as for the alkyl halides, as discussed above.

For the elimination reactions the situation is different. In this case the transition structures are also less strongly solvated than the reactant configurations. However, the trend in the solvation energies of the transition structures combined with the trend in the intrinsic barriers lead to the following trend in activation energies for the cluster models: $CH_3CH_2 > (CH_3)_2CH > (CH_3)_3C$. This is opposite to the trend for nucleophilic substitution.

Dostrovsky and Klein studied the competition between water exchange and dehydration of *tert*-butanol in weakly acidic aqueous solutions with isotopically labelled reactants.[67] They found that the ratio $k_{ex}/k_{dehyd} = 25$. Their data analysis is formally correct, but is in our opinion based upon a dubious mechanistic interpretation. It gives Arrhenius activation energies of 126 kJ mol^{-1} for exchange and 135 kJ mol^{-1} for dehydration. Our cluster models (last column of Table 2 and 3) reproduce the difference in the activation energy very well, but the absolute numbers are too low by 25%. A larger cluster model is probably needed to reproduce the experimental figures more accurately.

The experimental data and quantum-chemical models presented in this paper show how the intrinsic properties of the molecules affect reactivity. Despite the fact that these cluster models do not provide a complete picture of the situation in solution, it appears that the main features are described satisfactorily. This is strong evidence in favour of our proposition that the difference in the reactivity order between solution and the gas phase can be attributed to the differences in the interaction between nearest neighbours of the first solvation shell and the reacting unit in the TS and reactant configurations. The apparent difference between solution and gas-phase reactivity can only be accounted for by taking the effect of the solvent on the reactants and transition states into account. This is a well-known phenomenon. Most chemical properties (e.g., the relative acidities[68] and basicities[69] within a group of similar compounds) depend strongly on the environment of the molecules.

Conclusions

In this paper we have considered some key questions about the mechanisms of reactions between water and protonated alcohols in the gas phase and in clusters. The results also have implications for solution chemistry. Although we are careful not to carry our conclusions too far, some points are clear:

1) The reactivity orders for S_N2 substitution in the gas phase [calculated and experimental; $(CH_3)_3C > (CH_3)_2CH > CH_3 > CH_3CH_2$] and in solution [calculated; $CH_3 > CH_3CH_2 > (CH_3)_2CH > (CH_3)_3C$] are significantly different. This is an expression of solvent effects. The reactivity order in the gas phase for the reaction $H_2O + ROH_2^+ \rightarrow ROH_2^+ + H_2O$ is opposite to that found for the similar reaction $X^- + RY \rightarrow Y^- + RX$ and may not be explained by steric hindrance. Water, being a weak nucleophile is therefore seen to react differently from the halide anions, which are much stronger nucleophiles. The phrase steric hindrance—usually employed for describing properties of the substrate, and not the nucleophile—causes some confusion in this respect. We suggest that this term, when used, should be more precisely defined.

2) A gradual increase in the carbocationic character of key intermediate structures and transition structures along the series CH_3, CH_3CH_2, $(CH_3)_2CH$ and $(CH_3)_3C$ was observed. From the calculations it was observed that front-side substitution (S_N2_F with retention of configuration) competes better with back-side nucleophilic substitution (S_N2_B with inversion of configuration) with increasing stabilization of the carbocation. In the limit of highly stabilized carbocations, this may result in a situation in which the limiting S_N2_F and S_N2_B mechanisms merge into the S_N1 mechanism.

3) The cluster models appear to reproduce the solvent effects on elimination (E2) and substitution (S_N2).

Acknowledgments

The authors wish to thank VISTA (The Norwegian Academy for Science and Letters, and Statoil) for financial support and NFR (The Norwegian Research Council) for L.B.-A.'s scholarship and for generous amounts of computer time. Discussions with Professor Emeritus Johannes Dale have provided ideas and inspiration for this work. The authors are grateful to Professor John Brauman, Stanford University for providing the program HYDRA and for interesting discussions.

[1] W. H. Saunders, Jr., A. F. Cockerill, *Mechanisms of Elimination Reactions*, Wiley, New York, **1973**.
[2] T. H. Lowry, K. S. Richardson, *Mechanism and Theory in Organic Chemistry*, Harper and Row, New York, **1981**.
[3] F. Ruff, I. G. Csizmadia, *Organic Reactions. Equilibria, Kinetics and Mechanism*, Elsevier, Amsterdam, **1994**.

[4] N. Isaacs, *Physical Organic Chemistry*, Longman Scientific and Technical, Burnt Mill, Harlow, Essex, **1995**.
[5] W. A. Cowdrey, E. D. Hughes, C. K. Ingold, S. Masterman, A. D. Scott, *J. Chem. Soc.* **1937**, 1252.
[6] J. Dale, *J. Chem. Educ.* **1998**, *75*, 1482.
[7] S. Winstein, E. Clippinger, A. H. Fainberg, R. Heck, G. C. Robinson, *J. Am. Chem. Soc.* **1956**, *78*, 328.
[8] J. March, *Advanced Organic Chemistry*, Wiley, New York, **1985.**
[9] T. W. Bentley, C. T. Bowen, D. H. Morten, P. von R. Schleyer, *J. Am. Chem. Soc.* **1981**, *103*, 5466.
[10] T. W. Bentley, C. T. Bowen, *J. Chem. Soc. Perkin Trans. II* **1978**, 557.
[11] W. P. Jencks, *Chem. Soc. Rev.* **1982**, *10*, 345.
[12] I. Dostrovsky, E. D. Hughes, C. K. Ingold, *J. Chem. Soc.* **1946**, 173.
[13] T. W. Bentley, C. T. Bowen, W. Parker, C. I. F. Watt, *J. Am. Chem. Soc.* **1979**, *101*, 2486.
[14] P. Vogel, *Carbocation Chemistry*, Elsevier, Amsterdam, **1985**.
[15] W. Klopper, W. Kutzelnigg, *J. Phys. Chem.* **1990**, *94*, 5652 – 5630.
[16] J. E. Del-Bene, D. H. Aue, I. Shavitt, *J. Am. Chem. Soc.* **1992**, *114*, 1631.
[17] G. Olah, *Angew. Chem.* **1995**, *107*, 1519; *Angew. Chem. Int. Ed. Engl.* **1995**, *34*, 1393.
[18] S. S. Shaik, H. B. Schlegel, S. Wolfe, *Theoretical Aspects of Physical Organic Chemistry: The S_N2 Reaction*, Wiley New York, **1992**.
[19] V. I. Minkin, B. Y. Simkin, R. M. Minyaev, *Quantum Chemistry of Organic Compounds*, Springer, Berlin, **1990**.
[20] L. J. de Koning, N. M. M. Nibbering, S. L. van Orden, F. H. Laukien, *Int. J. Mass Spectrom. Ion Proc.* **1997**, *165/166*, 209.
[21] Y. Ikezoe, S. Matsuoka, M. Takebe, A. Viggiano, *Gas Phase Ion-Molecule Reaction Rate Constants Through 1986*, Maruzen, Tokyo, **1987**.
[22] M. J. Frisch, G. W. Trucks, H. B. Schlegel, P. M. W. Gill, B. G. Johnson, M. A. Robb, J. R. Cheeseman, T. A. Keith, G. A. Peterson, J. A. Mongomery, K. Raghavachari, M. A. Al-Laham, V. G. Zakrzewski, J. V. Ortiz, J. B. Foresman, J. Cioslowski, B. B. Stefanov, A. Nanayakkara, M. Challacombe, C. Y. Peng, P. Y. Ayala, W. Chen, M. W. Wong, J. L. Andres, E. S. Reploge, R. Gomperts, R. L. Martin, D. J. Fox, J. S. Binkley, D. J. Defrees, J. Baker, J. J. P. Stewart, M. Head-Gordon, C. Gonzalez, J. A. Pople, *GAUSSIAN 94*, Gaussian, Pittsburgh, PA, **1994**.
[23] P. C. Hariharan, J. A. Pople, *Theoret. Chim. Acta* **1973**, *28*, 213.
[24] M. J. Frisch, J. A. Pople, J. S. Binkley, *J. Chem. Phys.* **1984**, *80*, 3265.
[25] C. C. J. Roothan, *Rev. Mod. Phys.* **1951**, *23*, 69.
[26] C. Møller, M. S. Plesset, *Phys. Rev.* **1934**, *46*, 618.
[27] A. D. Becke, *J. Chem. Phys.* **1993**, *98*, 5648.
[28] A. P. Scott, L. Radom, *J. Phys. Chem.* **1996**, *100*, 16502.
[29] R. G. Gilbert, S. C. Smith, *Theory of Unimolecular and Recombination Reactions*, Blackwell Scientific, Oxford, **1990**.
[30] W. Forst, *Theory of Unimolecular Reactions*, Wiley-Interscience, New York, **1973**.
[31] B. D. Wladkowski, K. F. Lim, W. D. Allen, J. I. Brauman, *J. Am. Chem. Soc.* **1992**, *114*, 9136.
[32] K. Hiraoka, P. Kebarle, *J. Am. Chem. Soc.* **1977**, *99*, 360.
[33] K. Hiraoka, H. Takimoto, K. Morise, *J. Am. Chem. Soc.* **1985**, *108*, 5683.
[34] K. Raghavachari, J. Chandrasekhar, R. C. Burnier, *J. Am. Chem. Soc.* **1984**, *106*, 3124.
[35] S. G. Lias, J. E. Bartmess, J. F. Liebman, J. H. Holmes, R. D. Levin, W. G. Mallard, *J. Phys. Chem. Ref. Data* **1988**, *17*, 1.
[36] S. G. Lias, H. M. Rosenstock, K. Deard, B. W. Steiner, J. T. Herron, J. H. Holmes, R. D. Levin, J. F. Liebman, S. A. Kafafi, J. E. Bartmess, E. F. Hunter, *NIST Chemistry Webbook (http://webbook.nist.goc/chemistry),* **1997**.
[37] G. Caldwell, T. F. Magnera, P. Kebarle, *J. Am. Chem. Soc.* **1984**, *106*, 959.
[38] C. DePuy, S. Gronert, A. Mullin, V. M. Bierbaum, *J. Am. Chem. Soc.* **1990**, *112*, 8650.
[39] F. Jensen, *Chem. Phys. Lett.* **1992**, *196*, 368.
[40] S. Gronert, *J. Am. Chem. Soc.* **1993**, *115*, 652.
[41] C. N. Hinshelwood, K. J. Laidler, E. W. Timm, *J. Chem. Soc.* **1938**, 848.
[42] P. B. D. de la Mare, L. Fowden, E. D. Hughes, C. K. Ingold, J. D. H. Mackie, *J. Chem. Soc.* **1955**, 3169.
[43] A. Streitwieser, *Solvolytic Displacement Reactions*, McGraw-Hill, New York, **1962**.
[44] N. Ivanoff, M. Magat, *J. Chim. Phys.* **1950**, *47*, 914.
[45] E. Bauer, M. Magat, *J. Chim. Phys.* **1950**, *47*, 922.
[46] J. M. S. Henis, *J. Am. Chem. Soc.* **1968**, *90*, 844.
[47] J. L. Beauchamp, M. C. Caserio, *J. Am. Chem. Soc.* **1972**, *94*, 2638.
[48] J. L. Beauchamp, M. C. Caserio, T. B. McMahon, *J. Am. Chem. Soc.* **1974**, *96*, 6243.
[49] T. B. McMahon, J. L. Beauchamp, *J. Phys. Chem.* **1977**, *81,* 593.
[50] Z. Karpas, M. Meot-Ner, *J. Phys. Chem.* **1989**, *93*, 1859.
[51] L. M. Bass, R. D. Cates, M. F. Jarrold, N. J. Kirchner, M. T. Bowers, *J. Am. Chem. Soc.* **1983**, *105*, 7024.
[52] J. C. Kleingeld, N. N. M. Nibbering, *Org. Mass Spectrom.* **1982**, *17*, 136.
[53] J. C. Sheldon, G. J. Currie, J. H. Bowie, *J. Chem. Soc. Perkin Trans. II* **1986**, 941.
[54] D. G. Hall, C. Gupta, T. H. Morton, *J. Am. Chem. Soc.* **1981**, *103*, 2416.
[55] T. H. Morton, *Tetrahedron* **1982**, *38*, 3213.
[56] D. Berthomieu, H. Audier, *Eur. Mass Spectrom.* **1997**, *3*, 19.
[57] R. G. Keese, A. W. Castleman, *J. Phys. Chem. Ref. Data* **1985**, *15*, 1011.
[58] D. F. Shriver, P. W. Atkins, C. P. Langford, *Inorganic Chemistry*, Oxford University Press, Oxford, **1990**.
[59] E. Uggerud, *J. Am. Chem. Soc.* **1994**, *116*, 6873.
[60] G. Bouchoux, Y. Hoppilliard, *J. Am. Chem. Soc.* **1990**, *112*, 9110.
[61] D. J. Swanton, D. C. J. Marsden, L. Radom, *Org. Mass Spectrom.* **1991**, *26*, 227.
[62] R. P. Bell, *The Proton in Chemistry*, Chapman and Hall, London, **1973**.
[63] M. Meot-Ner, *J. Am. Chem. Soc.* **1984**, *106*, 1257.
[64] W. R. Davidson, J. Sunner, P. Kebarle, *J. Am. Chem. Soc.* **1979**, *101*, 1675.
[65] E. V. Waage, B. S. Rabinovitch, *Chem. Rev.* **1970**, *70*, 377.
[66] M. W. Wong, M. J. Frisch, K. B. Wiberg, *J. Am. Chem. Soc.* **1991**, *113*, 4776.
[67] I. Dostrovsky, F. S. Klein, *J. Chem. Soc.* **1955**, 791.
[68] J. E. Bartmess, J. R. T. McIver, in *Gas Phase Ion Chemistry*, *Vol. 2*, (Ed.: M. T. Bowers), Academic Press, New York, **1979**.
[69] J. L. Brauman, L. K. Blair, *J. Am. Chem. Soc.* **1970**, *92*, 5986.

Received: September 1, 1998 [F1333]

  0947-6539/99/0506-1930 $ 17.50+.50/0